Mantle convection with a brittle lithosphere: thoughts on the global tectonic styles of the Earth and Venus

Louis Moresi[1,2] and Viatcheslav Solomatov[3]

[1] *Research School of Earth Sciences, Australian National University, Canberra* ACT 0200, *Australia*
[2] *Australian Geodynamics Cooperative Research Centre, CSIRO Exploration & Mining,* PO Box 437, *Nedlands,* 6009 *Western Australia.*
E-mail: louis@ned.dem.csiro.au
[3] *Department of Physics, New Mexico State University, Las Cruces* NM 88003-8001, *USA. E-mail: slava@nmsu.edu*

SUMMARY

Plates are an integral part of the convection system in the fluid mantle, but plate boundaries are the product of brittle faulting and plate motions are strongly influenced by the existence of such faults. The conditions for plate tectonics are studied by considering brittle behaviour, using Byerlee's law to limit the maximum stress in the lithosphere, in a mantle convection model with temperature-dependent viscosity.

When the yield stress is high, convection is confined below a thick, stagnant lithosphere. At low yield stress, brittle deformation mobilizes the lithosphere which becomes a part of the overall circulation; surface deformation occurs in localized regions close to upwellings and downwellings in the system. At intermediate levels of the yield stress, there is a cycling between these two states: thick lithosphere episodically mobilizes and collapses into the interior before reforming.

The mobile-lid regime resembles convection of a fluid with temperature-dependent viscosity and the boundary-layer scalings are found to be analogous. This regime has a well defined Nusselt number–Rayleigh number relationship which is in good agreement with scaling theory. The surface velocity is nearly independent of the yield stress, indicating that the 'plate' motion is resisted by viscous stresses in the mantle.

Analysis suggests that mobilization of the Earth's lithosphere can occur if the friction coefficient in the lithosphere is less than 0.03–0.13—lower than laboratory values but consistent with seismic field studies. On Venus, the friction coefficient may be high as a result of the dry conditions, and brittle mobilization of the lithosphere would then be episodic and catastrophic.

Key words: brittle failure, lithosphere, mantle convection, non-linear rheology, temperature-dependent viscosity, viscoplastic rheology.

INTRODUCTION

The Earth appears to be unique among the terrestrial planets in having a mobile, actively deforming surface. Oceanic plates are created at mid-ocean ridges and destroyed by subduction. Early in the development of the theory of plate tectonics, Hess (1962) revived an idea originally proposed by Holmes (1931) that oceanic plates were the cold thermal boundary layer of convection in the mantle. Simple constant-viscosity convection models could explain the heat flow and depth–age relationships for the ocean floor (Turcotte & Oxburgh 1967); however, the surface motions associated with constant-viscosity convection are smoothly varying, quite unlike oceanic plates, which, to a good approximation, are rigid apart from narrow boundary zones (e.g. Minster & Jordan 1978; DeMets *et al.* 1990).

Laboratory measurements of the viscosity of mantle minerals tell us that the viscosity of the mantle is very far from being constant; it is a strong function of pressure, stress, composition and particularly temperature (Karato & Wu 1993). McKenzie (1977) and Davies (1988) showed that mantle convection using temperature-dependent viscosity produced a stiff upper boundary layer, but that the surface velocity was reduced and the distribution remained smooth. Since this work, thermo-viscous convection has been studied extensively and is now very well understood from a theoretical and modelling standpoint (Davaille & Jaupart 1994; Solomatov 1995), and from direct observation of laboratory experiments and lava lakes (Davaille & Jaupart 1993). According to this work, the viscosity of the cold lithosphere should be so high, even allowing for stress-dependent weakening, that surface motion

ought to be negligible (Solomatov 1995; Solomatov & Moresi 1997). Stagnant lid convection, as this mode is known, is a good description of the situation observed on Mars, Mercury, the Moon and probably Venus (Solomatov 1995; Solomatov & Moresi 1995), where the entire planetary surface is one continuous plate.

How can the surface of the Earth be mobile, and in what manner is the Earth different from the other terrestrial planets? The fact that earthquakes are strongly concentrated at the boundaries of the plates and the plate motions can be reproduced from slip directions (Isacks, Oliver & Sykes 1968) gives a very strong indication that plate tectonics is a product of the brittle failure of the cold lithosphere. Deformation in the brittle field is accommodated by slip on faults and cannot be described completely by a purely viscous fluid.

There have, however, been a number of different approaches to the introduction of plate-like surface flow into mantle convection models. Broadly, two different strategies have been employed. The first is to develop ways to model known plate structures and their influence on the mantle flow. For example it is possible to specify that certain regions must move in a plate-like manner either by imposing velocities (Hager & O'Connell 1981; Davies 1988; Lithgow-Bertelloni & Richards 1995) or by requiring regions to move coherently with velocity and rotation determined dynamically (Ricard & Vigny 1989; Gable, O'Connell & Travis 1991). Such models demonstrate that plate motions are determined by the distribution of buoyancy in the mantle and, conversely, that this buoyancy distribution is very strongly influenced by existing plate geometry. An alternative which does not impose rigidity of the plate interiors is to introduce weak zones in the coldest part of the computational domain to represent regions where brittle deformation, or non-linear weakening are expected to be dominant (Koptizke 1979; Schmeling & Jacoby 1981; Gurnis 1988; Davies 1989; King & Hager 1990). The logical development of these approaches is to introduce genuine discontinuities into the models to represent the locations of faults. This has been done globally for the major plate boundary faults by Bird (1997), although with highly simplified mantle dynamics, and for simplified fault geometries but fully consistent dynamical modelling by Zhong & Gurnis (1995, 1996).

If there is a problem with any of these models it is that the configuration of the plate boundaries is in some way specified, that is plates are not created or wholly consumed. A different modelling strategy aims to understand the underlying processes which lead to the formation of plates and plate boundaries in the first place, and to incorporate a description of this physics into a rheological model, thereby eliminating the need to specify a plate configuration *a priori*. The first approach was to use a non-Newtonian, temperature-dependent viscosity law in convection simulations with no imposed surface velocities as suggested by Cserepes (1982). Christensen (1983, 1984) showed that a temperature-dependent power-law rheology with exponent $n = 3$, as suggested by experimental data, led to more plate-like surface velocity distributions and larger aspect ratio convection cells than Newtonian viscosity. Weinstein & Olson (1992) extended this approach by constructing a non-Newtonian mantle/plate model consisting of a Newtonian convecting layer with a thin, very highly non-Newtonian layer at the surface. To obtain very localized zones of deformation they found it necessary to use power-law exponents larger than $n = 7$. They interpreted this strong non-linearity as a way

of parametrizing a highly faulted lithosphere. Bercovici (1993, 1995) studied a number of highly non-linear viscosity laws, using prescribed line sources and sinks in a plane, to determine the value of the power-law exponent which gives the highest degree of plate-like behaviour. Models with negative exponents, especially $n = -1$, were found to give the narrowest regions of deformation around the sources and sinks and narrow transform zones between them. This approach seems very successful at modelling convection with plate-like surface motions but it is not obvious how to progress into a physical picture once the best-fitting model is found, nor how to relate the best-fitting parameters to underlying physical properties of the lithosphere. It is also not obvious how such semi-empirical methods can be generalized to include, for example the more diffuse plate boundaries within continents, or to predict the behaviour of other planets. A more satisfactory strategy, perhaps, is that of Gurnis (1988), in which weak zones representing plate margins are reconfigured under explicit conditions of temperature and stress state.

In crustal deformation studies on scales of a few tens of kilometres down to a few metres, a more physical approach has been taken using principles from engineering studies of, for example localization of strain in deforming soils, metals and rocks. The technique is to use a viscoelastic–plastic rheology in which viscoelastic deformation occurs at relatively low stresses, but once a specific yield stress has been exceeded, the material deforms according to a plastic flow law. The theoretical basis for this approach is very well established and can be constrained by laboratory studies of engineering materials (e.g. as reviewed by Vermeer 1990). Applications include crustal-scale analysis of continental rifting and break-up (e.g. Braun & Beaumont 1987; Dunbar & Sawyer 1989), study of the planform of crustal deformation on a continental scale in response to mantle tractions and boundary forces using thin-skinned approaches (Bird 1989), the development of shear zones in compressional orogens (Beaumont, Fullsack & Hamilton 1994), and the development of shear bands in deformed rock masses (Poliakov & Herrmann 1994). Within this formulation, it is possible to parametrize the accumulation of damage within the medium (Lyakhovsky, Podlachikov & Poliakov 1993), which allows the natural development of shear zones into persistent weaknesses or, to all intents and purposes, faults (Ben-Avraham & Lyakhovsky 1992).

Is it possible to take the methods developed in regional crustal modelling and apply them to the larger-scale convection problem in which the mantle is also included in the solution process? The major obstacle is one of resolution (in both space and in time). Poliakov & Herrmann (1994) demonstrated that the distribution of shear bands in sheared rocks is fractal and, hence, that models' detailed results are resolution-dependent, but computations in coarser grids faithfully reproduce the larger-scale properties of the solution. A model which treats the mantle realistically will inevitably smooth out any developing shear bands near the surface to a scale of, perhaps, tens of kilometres. Such models will not capture any details of the brittle processes but ought to be able to describe the way in which brittle failure is induced by mantle stresses and couples back to influence the mantle flow field which generates these stresses. Instantaneous flow models using a similar rheology have been presented by Sleep (1975) for modelling the flow and stresses in subduction zones, and shown to reproduce the coarse-scale features of the system.

For this preliminary investigation, given the limitations imposed by the vastly different length scales present in the ductile versus the brittle layer, we restrict ourselves to the very simplest model of brittle failure in the lithosphere. We model the continuum limit in which it is assumed that the collective behaviour of a large set of randomly oriented faults can be described by a plastic flow law, and assume that it is not necessary to resolve individual faults. A further simplification casts this assumption in the form of a transition to a different viscous rheological law when the yield stress is reached, which allows the use of the fast non-linear viscosity algorithm.

This approach gives considerable insight into the coupling between the brittle lithosphere and the viscous convecting mantle. We are able to estimate the conditions under which forms of convection with a mobile upper surface may occur, and find that they are in reasonable agreement with observations from the Earth.

GOVERNING EQUATIONS AND NUMERICAL METHOD

We solve Stokes' equation for creeping flow subject to incompressibility:

$$-\nabla(\eta \boldsymbol{D}) + \nabla p = \Delta \rho g \hat{\boldsymbol{z}}, \tag{1}$$

$$\nabla \cdot \mathbf{u} = 0, \tag{2}$$

in which η is the dynamic viscosity, $\boldsymbol{D}_{ij} = (\partial u_i/\partial x_j + \partial u_j/\partial x_i)$ is the strain rate tensor, p is the dynamic pressure, $\Delta \rho$ is the density anomaly, g is gravitational acceleration, $\hat{\boldsymbol{z}}$ is a unit vector pointing downwards, and $\mathbf{u}$ is the velocity. These equations are solved by the CITCOM finite element code (Moresi & Solomatov 1995) which uses a multigrid solver for the equation of motion, coupled to the continuity equation via a multigrid Uzawa iteration. Non-linear viscosity is solved by repeated substitution at each multigrid level of the Uzawa iteration which results in a very fast, robust numerical scheme.

The energy equation describes the evolution of the temperature field:

$$\frac{\partial T}{\partial t} = \kappa \nabla^2 T - \mathbf{u} \cdot \nabla T, \tag{3}$$

in which κ is thermal diffusivity. It is solved using explicit timestepping of a Petrov–Galerkin upwind method (Brooks & Hughes 1982).

The following changes of variables are made throughout to non-dimensionalize all quantities:

$$t = \frac{d^2}{\kappa} t' \qquad x_i = d x_i' \qquad u_i = \frac{\kappa}{d} u_i',$$

$$\eta = \eta_0 \eta' \qquad \tau = \frac{\eta_0 \kappa}{d^2} \tau' \qquad T = \Delta T T', \tag{4}$$

where t is time, d is the layer depth, η_0 is a reference viscosity, τ is stress, and ΔT is a reference temperature drop across the system. From this point, variables are assumed to be non-dimensional and primes are omitted.

The system is characterized by a Rayleigh number, Ra_0, defined using the basal viscosity, η_0, and a Rayleigh number, Ra_i, based on a characteristic viscosity for the system. There is no unique definition for this characteristic viscosity but it is generally considered useful to choose an average which represents the viscosity of the actively convecting part of the fluid:

$$Ra_{\{0,i\}} = \frac{g \rho \alpha \Delta T d^3}{\kappa \eta_{\{0,i\}}}, \tag{5}$$

in which α is the thermal expansivity and g is the gravitational acceleration. The interior viscosity, η_i, can be determined either geometrically by assuming typical boundary layer thicknesses and temperature drops (Torrance & Turcotte 1971; Booker 1976; Nataf & Richter 1982) or by computing, from a full simulation, a strain-rate-averaged value of the viscosity (Parmentier, Turcotte & Torrance 1976; Christensen 1984).

RHEOLOGY OF MANTLE AND LITHOSPHERE

Different deformation mechanisms are expected to be active at different pressures, temperatures and stresses in the mantle (Karato & Wu 1993). The dominant effect is, however, the temperature, and this influences the viscosity as follows:

$$\eta(T) = B \exp\left(\frac{Q}{RT}\right), \tag{6}$$

where T is the temperature, B is a constant, Q is an activation energy and R is the gas constant. Comparisons with boundary layer approximations are greatly simplified if the rheological law is decomposed and approximated by an exponential function following Frank-Kamenetskii (1969):

$$\eta = \exp(-\theta T), \tag{7}$$

where $\theta = Q \Delta T / T_i^2$, and T_i is the temperature of the hot interior of the convecting system. A detailed explanation of the range of applicability of this approximation is given in Solomatov & Moresi (1995). A useful quantity in characterizing the system is the viscosity change associated with the temperature drop across the layer:

$$\Delta \eta = \exp(\theta). \tag{8}$$

The coldest parts of the lithosphere are in the brittle regime in which deformation can occur through slip on faults. This behaviour can be modelled in the continuum limit (where individual faults are not resolved) by assuming a viscoplastic rheology in which viscous deformation occurs when the second invariant of the stress tensor falls below a yield value, τ_{yield}, but, when stresses reach this value, further deformation occurs according to a plastic flow law such that τ_{yield} is never exceeded in the material (that is stresses always fall within a failure envelope).

At this point we are faced with a choice: we can explicitly define a plastic flow law which determines strain rates during plastic deformation, or we can model plastic deformation using a non-linear effective viscosity which is adjusted to ensure the stresses remain bounded by the failure envelope (for discussion see Fullsack 1995). We are mainly concerned with the influence of a brittle upper lithosphere on the large-scale features of mantle convection; we do not expect to be able to resolve localized features of plastic deformation within very large-scale convection problems. In this context, the formulation of plastic deformation via an effective viscosity is sufficient. Furthermore, since we are working within an incompressible formulation designed for predominantly viscous flow, we cannot include the effects of dilatation which occurs if the yield criterion is a general function of pressure. With this point in mind, we define

the yield criterion from Byerlee's frictional law (Byerlee 1968) in which we have assumed the normal stress to be independent of the dynamic pressure:

$$\tau_{\text{yield}} = c_0 + \mu \rho g z, \tag{9}$$

where c_0 is a yield stress at zero hydrostatic pressure (the cohesive limit) and μ is a frictional coefficient. The non-dimensional form of the equation is

$$\tau'_{\text{yield}} = \tau_0 + \tau_1 z', \tag{10}$$

where the cohesion term τ_0 is given by

$$\tau_0 = \frac{d^2}{\kappa \eta_0} c_0, \tag{11}$$

and the non-dimensional depth-dependent term is

$$\tau_1 = \frac{\mu \rho g R a_0}{\alpha \Delta T}. \tag{12}$$

The non-linear effective viscosity for the plastic deformation is given by

$$\eta_{\text{yield}}(D) = \frac{\tau_{\text{yield}}}{D}, \tag{13}$$

in which D is the second invariant of the strain rate tensor. Combining each of the possible deformation mechanisms and introducing a branch for plastic behaviour gives the following rheological law for the system:

$$\eta = \begin{cases} \eta_{\text{creep}} & (\tau_{\text{creep}} < \tau_{\text{yield}}) \\ \eta_{\text{yield}} & (\tau_{\text{creep}} \geq \tau_{\text{yield}}) \end{cases}, \tag{14}$$

where τ_{creep} is the stress invariant obtained using solely the purely viscous rheology. Because the stresses are determined during the course of the iteration, it is possible for the system to hunt between viscous and plastic branches from one iteration to the next. This has little influence on the large-scale velocity field but it is sometimes hard for the algorithm to judge whether convergence has been achieved. A way to eliminate the hunting across the transition, which we found to be very effective, is to introduce a small amount (<0.1 per cent) of hysteresis into the branching. To do this we need to keep track of where the material is deforming plasticly. This can be achieved at no additional storage cost by tagging values of viscosity obtained while on the plastic branch as negative numbers. Note, however, that there is no underlying physical property of the material which is assumed to be responsible for this hysteresis because it is not advected with the flow. In principle, tracking the yield behaviour during the iteration allows us to introduce rheologies in which deformation after yielding occurs at decreasing stress as a function of strain rate. Given the limits of our modelling of plastic deformation discussed earlier, we consider it premature to explore this avenue in this paper.

CONVECTION WITH TEMPERATURE-DEPENDENT VISCOSITY

Mantle convection with temperature-dependent viscosity has been thoroughly investigated theoretically (e.g. Morris & Canright 1984; Fowler 1985b; Davaille & Jaupart 1994), experimentally (e.g. Nataf & Richter 1982; Davaille & Jaupart 1993) and numerically (e.g. Christensen 1983, 1984; Tackley

1993; Moresi & Solomatov 1995; Ratcliff, Schubert & Zebib 1995) and is now well understood. When the viscosity is mildly temperature-dependent, convection cells resemble the constant-viscosity situation: top and bottom boundary layers are similar in thickness, and the upper boundary layer is mobile. As viscosity becomes more strongly dependent on temperature, the cold, upper boundary layer becomes relatively thicker and more sluggish. Eventually, the coldest part of the fluid becomes so viscous that it does not take part in the flow, and convection occurs beneath a stagnant lid (Fig. 1a).

The temperature dependence of the viscosity of mantle rocks is so strong that, if deformation occurred by viscous processes alone, the Earth would fall firmly into the stagnant lid convection regime like Mars, Mercury, the Moon and possibly Venus. This conclusion is not affected by consideration of the stress dependence of the viscosity of mantle materials because the temperature dependence dominates (Solomatov & Moresi 1997).

MOBILIZATION OF THE LITHOSPHERE BY BRITTLE FAILURE

Fowler (1985a) recognized that brittle failure, modelled in the continuum limit by plastic flow, might permit the stagnant lid to become mobile by weakening it in the vicinity of incipient downwellings. This would, perhaps, lead to a mode of convection reminiscent of plate tectonics in which the upper layer is very viscous but moves with velocities comparable to the low-viscosity interior and deformation at the surface occurs in relatively narrow zones.

Stresses in the stagnant lid are highly concentrated within a narrow stress 'skin' which lies close to the free surface. High stresses at shallow depths imply that this region is where plastic deformation is expected to occur when a yield criterion is introduced. Fowler argued that the stagnant lid could be mobilized if the plastically deforming region extended all the way to the base of the lid at some point. This argument is most applicable to the initiation of subduction in a system which has an existing stagnant lithosphere. Because the thick stagnant lid is required to generate the high stresses which induce plastic flow, it is not obvious whether the new state (with a thinner, mobile lid) will be transient or truly self-sustaining.

Does localized failure within the lithosphere result in a different convective style with long-lived, viscous 'plates' actively participating in the large-scale flow? To address this question, and to characterize the nature of convection in this coupled system, we now turn to numerical experiments.

Regimes of convection with brittle lithosphere

In fact, we find that there is competition between the tendency for the thermally activated rheology to produce a stagnant lid and for plastic flow at high stresses to mobilize this lid. Not surprisingly this leads to distinct regimes of behaviour. In one end-member, viscosity dominates over plasticity. This is, essentially, the familiar stagnant lid regime illustrated in Fig. 1(a), characterized by a thick upper boundary layer and very small surface velocities. In the other end-member, plastic flow occurs at low enough stresses for the lid to become permanently mobile (Fig. 1b), with a velocity comparable to the interior velocity. Convection in this regime is very similar to constant-viscosity convection with a similar Nusselt number
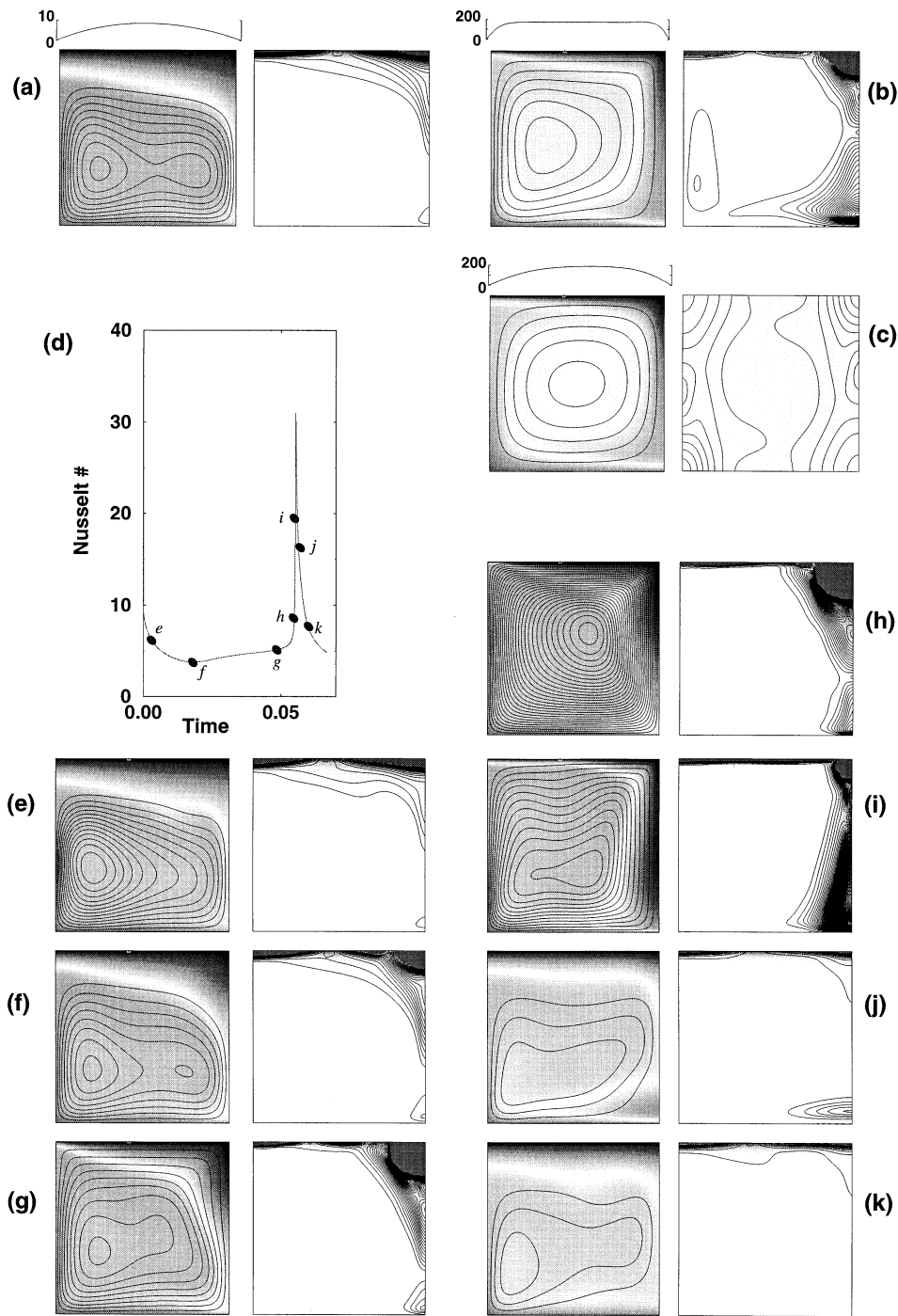
Figure 1. Three regimes of convection with strongly temperature-dependent rheology and a brittle lithosphere. Temperature plots (darkest colours are coolest) and streamfunction contoured at a fixed interval of 10.0, and stress contoured at intervals of 5×10^4 with plastically deforming region highlighted: $Ra = 10^7$, $\Delta\eta = 3 \times 10^4$, $\tau_1 = 10^7$. (a) The familiar stagnant-lid regime ($\tau_0 = 10^6$). (b) Plasticity dominated mobile-lid regime ($\tau_0 = 10^5$). (c) Constant-viscosity convection with the same Nusselt number as (b). The thickening and collapse of the stagnant lid in the episodic overturn regime ($\tau_0 = 5 \times 10^5$) is detailed in (d)–(k). (d) Nusselt number as a function of time; the circles indicate the time of each of the snapshots in (e)–(k).

(Fig. 1c) except that the surface velocity is very flat away from the cell boundaries, where viscosity remains high. Finally, there is an intermediate regime in which there is time-dependent competition between the two end-members. This regime is characterized by episodic, catastrophic collapse of a stagnant lid followed by quiescence when the upper boundary layer cools, thickens and once again becomes stagnant (Figs 1e–k).

Transient behaviour: collapse of the stagnant lid

We examine in some detail the manner in which the stagnant lid fails in the episodic regime and during transient adjustments in systems which eventually settle down to mobile or stagnant lids. This has a bearing on Fowler's viscoplastic theory for the initiation of subduction in a previously stagnant convection

cell. A direct comparison with this theory is not possible because it assumes a von Mises yield criterion which has no depth dependence. In such experiments in the episodic or mobile-lid regimes, we found that the stresses in the actively convecting interior would exceed the yield criterion at some point in the simulation and a runaway would ensue. (This is expected because the interior stresses must be comparable to the upper boundary layer stresses in order to mobilize the lid).

Snapshots of a stagnant lid undergoing collapse are shown in Figs 1(e)–(k). Fig. 1(d) shows the Nusselt number during this cycle, and the times of each snapshot are indicated. Regions where plastic deformation occurred are highlighted in the viscosity/stress plots. Initially (e), the boundary layer was relatively thick and deformed slowly, stresses in the lid were concentrated near to the surface, and plastic deformation was limited to no more than a third of the total boundary layer thickness. As the lid continued to thicken, plastic deformation became more important above the downwelling, and the lid slope began to increase (f). These changes in the lid geometry meant that plastic deformation in the boundary layer above the upwelling became the dominant mode and necking occurred, mobilizing the entire cold thermal boundary layer (g). The resulting collapse was catastrophic as the gravitational potential energy of the stagnant lid was released in a very short interval (h,i), and the Nusselt number and surface velocity increased dramatically. However, as the detached boundary layer sank, it encountered resistance from the bottom boundary and slowed down. This material then formed a cold blob on the lower boundary, and was gradually removed by heating from below (j). The Nusselt number declined and the stagnant lid began to reform (k). The behaviour was cyclic with some long-period variations and, in this particular case, after about 10 over-turns (depending on initial conditions) the intensity of the overturns began to decay and a stagnant lid developed. In other cases the episodic behaviour showed no signs of decaying to mobile-lid or stagnant-lid convection irrespective of initial conditions.

Catastrophic failure occurs when the integrity of the stagnant lid is interrupted by the region of plastic deformation above the upwelling limb of the cell (g). This differs from Fowler's calculation based on the von Mises criterion in which failure occurs close to the downwelling. The use of Byerlee's law to define a yield criterion, together with fully dynamical model-ling, thus suggests that distant regions of weakness where the lithosphere can rift may have a strong, even controlling, influence on the foundering of old, cold, stagnant lithosphere.

Nusselt numbers and surface velocities for three regimes of viscoplastic behaviour

For the stagnant-lid and mobile-lid regimes at moderate Rayleigh number, the convection cell settles to a steady state and we can characterize the behaviour relatively quickly. However, in order to characterize the episodic-overturn regime (e.g. to find average Nu) we need to follow the system through several episodes. This can be very time consuming so we ran tests to determine the coarsest reliable mesh to use for the computations. For the cases modelled here, we found that a 32×32 element mesh gave reliable Nusselt number, surface velocity and rms velocity estimates (within 1.1, 2.0, 6.3 per cent respectively of the values from a 64×64 element mesh in the stagnant-lid regime, and 0.6, 0.5, 1.7 per cent in the mobile-

lid regime) provided grid refinement in the upper and lower boundary layers was used. The Nusselt number, surface and rms velocity spikes of the episodic regime were resolved to within 1.0, 4.3, 4.5 per cent. The coarser grid tended to blur the boundaries of the different regimes by inducing low levels of oscillatory behaviour in an imperfectly resolved plastic region. There were some differences in the rms velocity (associated with small-scale instabilities in the lower boundary layer) between coarser and finer grid runs, but the overall cyclic behaviour was well resolved, including the interval between overturns (Fig. 2). Our approach was to use a 32×32 element mesh to map the behaviour for a wide range of parameters and then run on a 64×64 element mesh to study the detailed behaviour for the range of interest.

Fig. 3 shows Nu and surface velocity plotted against time for Rayleigh number 10^7, $\Delta\eta = 3 \times 10^4$, $\tau_1 = 10^7$ for three values of τ_0 (10^5, 4×10^5, 10^6) which correspond to mobile-lid, episodic-overturn and stagnant-lid regimes respectively. The starting point was a constant-viscosity calculation at the same Rayleigh number (based on bottom viscosity) which has a significantly thinner initial boundary layer than the equilibrium value for any of these calculations. The mobile lid run under-went some oscillations before settling into a steady state with high Nusselt number, and a surface velocity comparable to the interior velocity—this condition was chosen because the formation of a thick lid from a thin lid is much less violent and time consuming than the shedding of an initially thick boundary layer. The stagnant-lid run rapidly decayed to low Nusselt number and very low surface velocity. The episodic case initially tracked the stagnant-lid run before, eventually, the lid collapsed. This made it time consuming to determine the boundary between the stagnant-lid and episodic-overturn regimes: it was necessary to observe a number of overturns to see if they were dying away. Note how the episodic behaviour resulted in surface velocity and Nusselt numbers which over-shot the mobile-lid values and also undershot the stagnant-lid values. The mean value of Nusselt number for runs in which the lid overturned was usually very similar to that obtained for mobile-lid convection with the same Rayleigh number and viscosity contrast.

The results of an exploration of the parameter space are summarized in Fig. 4. Time-averaged Nusselt numbers are plotted for a sweep of τ_0 for different values of RA, $\Delta\eta$ and τ_1. Fig. 4(a) is the standard suite and includes the runs discussed above. The different behavioural regimes are indicated by the horizontal bars. An arctangent curve was fitted to the data to illustrate the sharpness of the transition to stagnant-lid behaviour. Lowering the value of τ_1 (Fig. 4b) to 10^6 shifted the location of the transition to higher τ_0 and slightly broadened this transition but had a minimal effect on the Nusselt number of the mobile-lid regime, which increased modestly from 10.7 to 11.1. In Fig. 4(c), the viscosity contrast due to temperature was increased to 10^6. This decreased all Nusselt numbers and, by virtue of there being a thicker, stronger lid, the transition to mobile-lid behaviour required a lower τ_0. Furthermore, in this case, the transition was directly from steady mobile lid to steady stagnant lid with no evidence of persistent episodicity. Finally, we ran a set of calculations at a lower Ra of 10^6 (Fig. 4d). As a result of the non-dimensionalization, in order to maintain constant μ, we reduced the value of τ_1 in line with Ra. The transition to mobile-lid convection occurred at an order of magnitude lower stresses than in Fig. 4(a). Nusselt
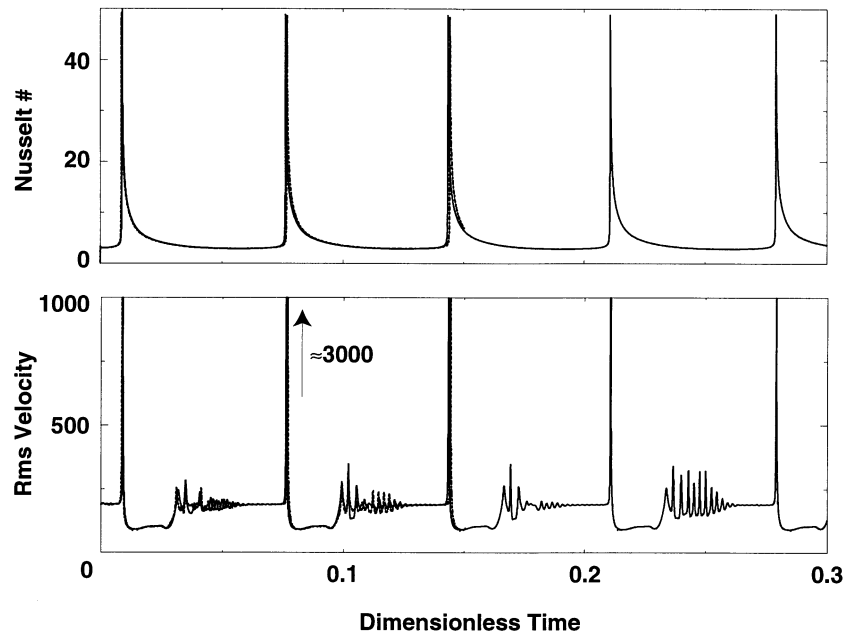
© 1998 RAS, *GJI* **133,** 669–682

Figure 2. Benchmark comparison of episodic overturns with large viscosity contrast at different grid resolutions: 32×32 elements (solid line) and 64×64 elements (dotted line). 50 per cent grid refinement was used in both cases close to the upper and lower boundaries. $Ra = 10^7$, $\Delta\eta = 10^6$, $\tau_1 = 7 \times 10^5$, $\tau_0 = 3 \times 10^5$.
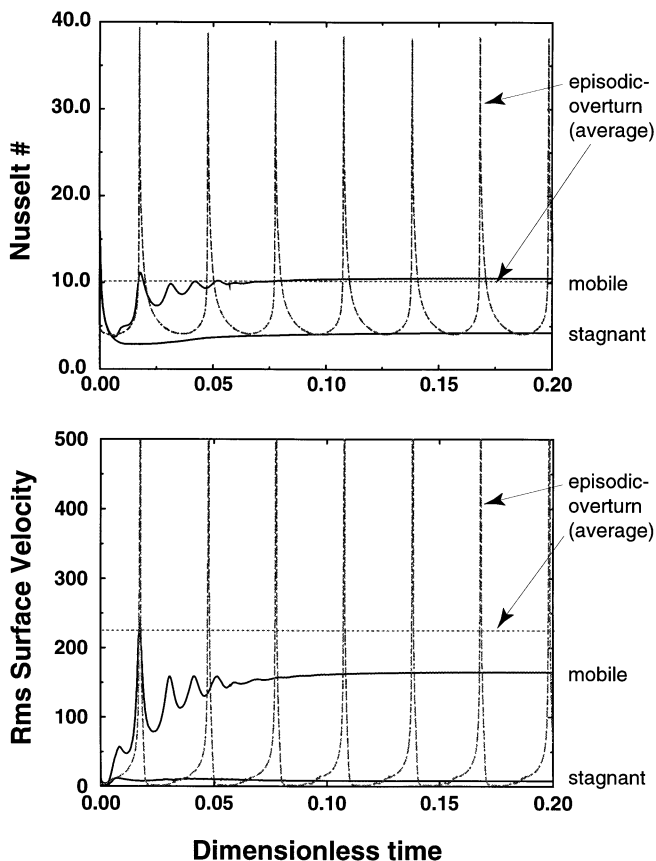

Figure 3. Nusselt numbers and surface velocities over time for the mobile-lid, episodic-overturn and stagnant-lid regimes. $Ra = 10^7$, $\Delta\eta = 3 \times 10^4$, $\tau_1 = 10^7$, $\tau_0 = 10^5$, 4×10^5, 10^6, respectively.

numbers were generally low: the mobile lid was relatively slow and thick; the stagnant lid became particularly thick. This led to initial episodic collapses of the stagnant lid eventually dying away to steady stagnant behaviour after a long time ($t \approx 1$). Fig. 4(e) shows a log plot of time-averaged rms surface velocity for the transitions illustrated in Figs 4(a) and (c). Again, an arctangent function was fitted through the data to illustrate the sharp nature of the transition. The mean surface velocity associated with the episodic-overturn cases was larger than found in the mobile lid, which is indicative of the enormous velocities associated with foundering of the upper boundary layer. The stagnant-lid velocity is controlled by the overall viscosity contrast and, for sufficiently high τ_0, agrees with the values determined by Moresi & Solomatov (1995). The case of a viscosity contrast of 3×10^4 is located just beyond the transition to the stagnant-lid regime (very low viscous dissipation in the lid) and the surface velocities reflect this.

Most notable about the plots of Fig. 4 is that the curves are very flat within each regime. Nusselt number and surface velocity are nearly independent of the yield criterion on either side of the transition. This is not surprising for the stagnant lid case where little or none of the lid is affected by plastic flow, but in the mobile-lid regime it indicates that the surface velocities are not controlled by the exact details of the weak zones which develop at their edges, and, therefore, are not controlled by the deformation at the converging or diverging part of the boundary layer. Extending this argument to the Earth, the implication is that the plate velocities are limited by the resistance of the mantle rather than by the frictional resistance of subduction zones.

Scaling laws for mobile-lid convection

Having established that the mobile-lid regime has a well-defined Nusselt number independent of the exact nature of the yield criterion, we now attempt to determine the dependence
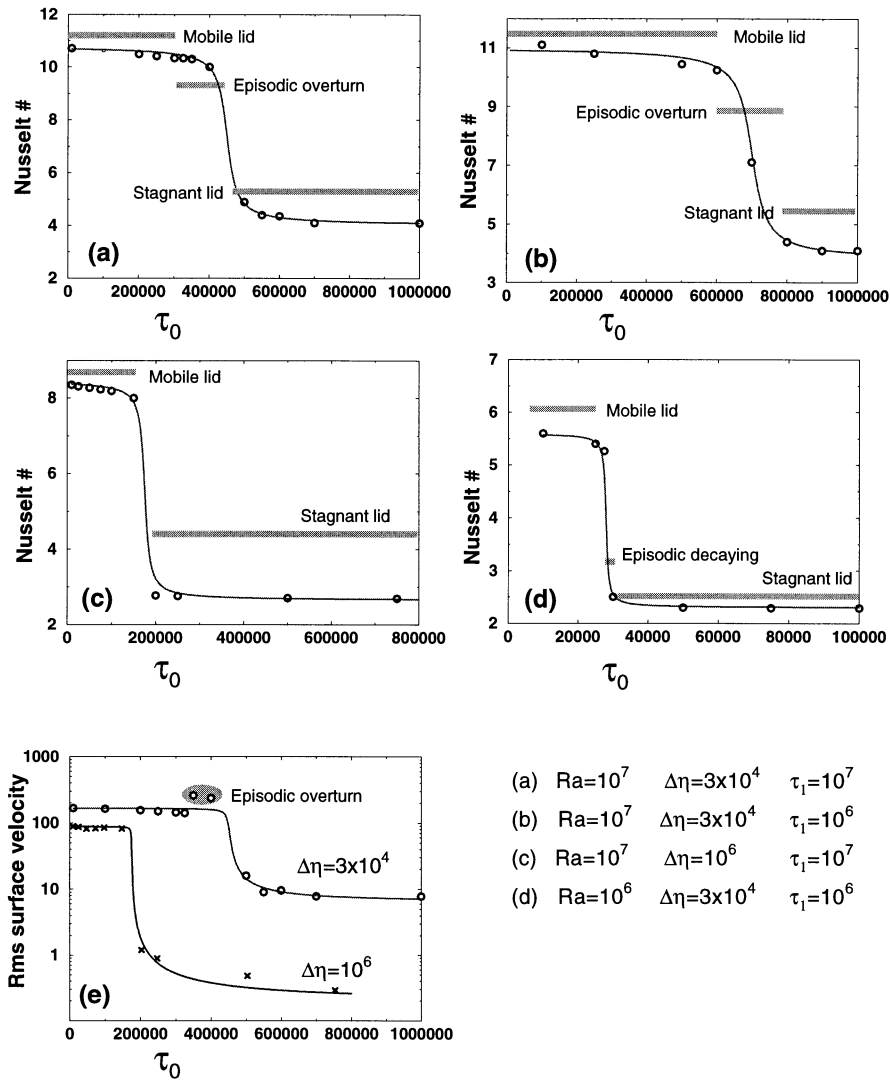
Figure 4. The transition from mobile-lid convection to stagnant-lid convection as a function of the yield stress parameter τ_0. (a) The reference model incorporating data shown in Figs 1 and 3. The effect on Nusselt number of (b) reducing the friction coefficient, μ, (c) increasing the viscosity contrast, $\Delta\eta$, (d) lowering the Rayleigh number, Ra. Surface velocities are plotted in (e) for data from (a) and (c).

of this Nusselt number on the Rayleigh number and viscosity contrast. Olson & Corcos (1980) suggested that the relationship

$$Nu \sim Ra_i^{1/3} \tag{15}$$

might apply to convection with mobile plates. The interior viscosity for the small-viscosity-contrast regime (which also has a mobile upper boundary layer) has been determined experimentally (Torrance & Turcotte 1971; Booker 1976; Nataf & Richter 1982) to be approximately

$$\eta_i \approx \eta(\Delta T/2), \tag{16}$$

which, in our case, means that (15) can be written in the form

$$Nu \sim Ra_0^{1/3} \exp(\theta/6). \tag{17}$$

This second relationship is taken as our starting point because Ra_i and η_i are not known *a priori*.

We ran unit aspect ratio calculations for a range of Rayleigh numbers (10^5–10^8) and viscosity contrasts (10^4–10^8), choosing a yield stress for each case which was low enough to ensure the system was far away from the transition to stagnant

lid convection. However, at low Rayleigh number and high viscosity contrast, we were not able to obtain steady, mobile-lid convection due to the effective Rayleigh number for viscous convection being subcritical. At very high Rayleigh number, and large viscosity contrast, we faced problems of convergence in the numerical method.

The results from 15 runs are plotted in Fig. 5(a); open symbols represent cases where the system remained periodic, but had reached a statistically steady state. The Nusselt number was found to be much more strongly dependent on the Rayleigh number than on viscosity contrast, as anticipated from (15). The least-squares fit to this data gave the following relationship:

$$Nu \approx 0.582 Ra_0^{0.224} \exp(\theta/15.36). \tag{18}$$

The lines shown in Fig. 5(a) and the plot of actual against estimated Nusselt number in Fig. 5(b) were obtained from (18). The fit to the data was reasonable, although it underestimated the higher Nusselt numbers, but the power-law exponents were very different from the predicted values. This was largely because the estimate of the interior viscosity was
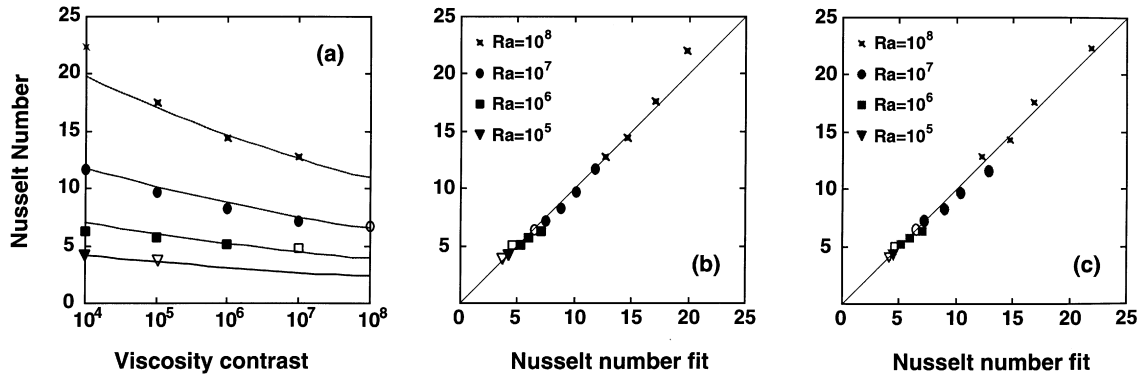
Figure 5. (a) Nusselt number–Rayleigh number–viscosity contrast relations for the mobile-lid regime. Data were obtained where possible for viscosity contrasts from 10^4 to 10^8, and at Rayleigh numbers from 10^5 to 10^8, choosing a weak yield criterion to be on the flat part of the curve (see Fig. 4). Symbol shapes denote Ra, open symbols mean there was residual time dependence. (b) Fitting of the Nusselt number to theoretical relationship. (c) Fitting to a power-law relationship of effective Ra based on measured effective viscosity.

so simple, being based on the value $\eta(T = 0.5)$. On the assumption that the mean viscosity is a function of both Ra and overall viscosity contrast, we obtained the following expressions for the interior viscosity and Nusselt number based on this viscosity:

$$\eta_i \approx 0.147\eta_0 Ra_0^{0.245} \exp(\theta/3.96), \tag{19}$$

$$Nu \approx 0.385 Ra_i^{0.293}. \tag{20}$$

The exponent in the power-law relationship between Nusselt number and Rayleigh number based on the interior viscosity was in much better agreement with the theoretical prediction of 1/3 (Fig. 5c).

Conditions for mobile-lid convection

It is interesting to estimate the conditions required for the lid to be permanently mobilized as these underlie the ability of a planet to maintain plate tectonics. A general condition for the lid to become, and remain, mobile is that the yield stress is always exceeded at the edges of the moving cold boundary layer. In the steady state, we observed that the velocity of the upper boundary layer is controlled by the interior viscosity, so the appropriate stress scale is:

$$\tau \sim \frac{\eta_i u_0}{d}, \tag{21}$$

in which the upper boundary layer velocity, u_0, is (from the energy equation)

$$u_0 \sim \frac{\kappa d}{\delta_0^2}, \tag{22}$$

where δ_0 is the upper boundary layer thickness which we determine from the Nusselt number ($\delta_0 \sim d\mathrm{Nu} \sim d\mathrm{Ra}_i^{-1/3}$). Substituting (22) into the stress scaling, and writing in a non-dimensional form (using eq. 4) gives

$$\tau \sim \frac{\eta_i d^2}{\eta_0 \delta_0^2}. \tag{23}$$

We can now estimate upper bounds on τ_0 and τ_1 for the mobile-lid style of convection to be possible. Ignoring depth dependence initially, we determine that the cohesion term, τ_0, must satisfy

$$\tau_0 \leq \omega_0 \frac{\eta_i}{\eta_0} Ra_i^{2/3}, \tag{24}$$

where the constant factor ω_0 accounts for the uncertainties in the scaling relationships. Similarly, if we ignore τ_0, an upper bound for τ_1 can be obtained. In this case, however, it is necessary to specify a length scale over which the average yield stress exceeds the convective stresses. A suitable choice is the boundary layer thickness, δ_0, which gives

$$\tau_1 \delta_0/d \leq \omega_1 \frac{\eta_i d^2}{\eta_0 \delta_0^2} \Rightarrow \tau_1 \leq \omega_1 Ra_0, \tag{25}$$

where, again, a constant factor, ω_1, is included to account for the approximate nature of the scaling laws. This relationship is remarkably simple and leads to a further surprising result if we now return to the dimensional variables to determine a bound on the friction coefficient:

$$\mu\rho g\delta_0 \leq \omega_1 \frac{\eta_i \kappa}{\delta_0^2} \Rightarrow \mu \leq \omega_1 \alpha\Delta T. \tag{26}$$

Thus mobilization of the surface boundary layer may simply be a matter of having a sufficiently low friction coefficient.

As we noted previously, the fact that the internal convective stresses dominate the mobile lid convection regime means that it is generally very difficult to run simulations with small τ_1 and it is therefore difficult to obtain a value for ω_0. On the other hand, the only difficulty when $\tau_0 = 0$ is that the viscosity gradients in the topmost row of elements become enormous once yielding occurs. If the yield stress is truncated so that it is constant in the topmost row of elements then it is possible to estimate a value for ω_1.

The results of a number of runs with no cohesion are shown in Fig. 6. The transition to mobile-lid convection occurred over a very narrow range of ω_1 between 1.25 and 1.75. There was good agreement with the theoretical prediction of (26) that neither the Rayleigh number nor the viscosity contrast are important in determining the location of the transition, provided convection is sufficiently vigorous for the boundary layer approximations to be valid. We did not attempt to obtain a best-fit value of ω_1 from our experiments because the transition to the mobile-lid regime is not particularly sharp, and depends slightly on the initial conditions—under these circumstances a range of the critical value of the coefficient ω_1 appears to be most useful.

Using this range of ω_1, we can estimate the maximum value of μ which allows mobile-lid convection in the Earth.
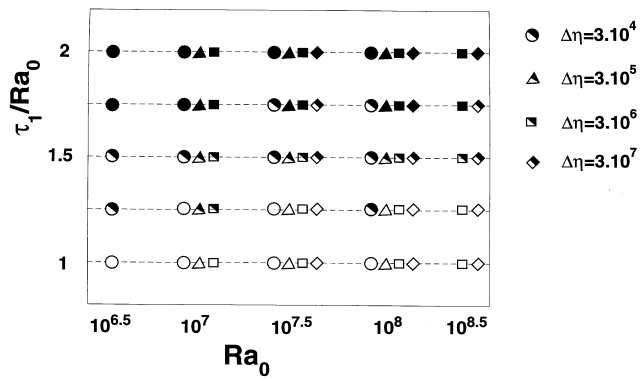
Figure 6. The transition to mobile-lid convection as a function of the depth-dependent yield stress for a range of Rayleigh numbers and viscosity contrasts. Solid symbols indicate stagnant-lid or episodic-overturn behaviour, open symbols indicate a fully mobilized lid. Close to the transition, it can be difficult to discern which regime best characterizes the system, and these cases have been marked by half-filled symbols.

Internal heating is the dominant source of energy for convection in the Earth, so the appropriate thermal expansivity and reference temperature values to use in eq. (26) are those which best apply to subducting slabs where buoyancy anomalies are concentrated—approximately we can assume upper-mantle conditions. The thermal expansivity of mantle materials at realistic mantle pressures has been measured by Chopelas & Boehler (1989) and for the upper mantle ranges between 2×10^{-5} and 5×10^{-5}. The system temperature drop must lie somewhere between the reference potential temperature of the mantle obtained from mid-ocean ridge crust production rates (1280°C, McKenzie & Bickle 1988) and the maximum potential temperature of mantle plumes (1600°C, White 1993). This leads to a range for the critical value of μ between 0.03 and 0.13. It is worth noting, however, that this friction coefficient is applicable to the continuum representation of a lithosphere with multiple faults, and is obtained with reference to an effective viscosity, and this is a source of further uncertainty in applying this criterion for mobile-lid convection to the Earth or to Venus.

Large aspect ratio study

In the unit aspect ratio domain there is always the concern that the restriction of the horizontal length scale can have a significant influence on the flow pattern. This concern becomes even more acute when we are trying to mimic the behaviour of the lithospheric plates, since they are typically associated with large aspect ratio flow.

Consequently, we next consider archetypal examples from each of the regimes, this time using significantly wider boxes (4×1). We re-examined the three cases used in Fig. 3 to illustrate the behaviour of each of the different regimes of behaviour. As before, the initial condition was a constant-viscosity convection solution at the same Rayleigh number (using basal viscosity) and with unit aspect ratio cells. This initial solution was also perturbed by adding a harmonic disturbance to the temperature field as follows:

$$T \leftarrow T + \sin(\pi z/d)[0.05 \cos(\pi x/2d) + 0.01 \cos(\pi x/4d)]. \quad (27)$$

The mobile-lid case (Fig. 7(a), $\tau_0 = 10^5$) continued with unit aspect ratio cells for a considerable period of time and approached the same solution as was obtained in the 1×1 box. At $t = 0.05$ (arrow 1) the original perturbation was reapplied and the convection cells began to reorganize. The pair of downwellings began to migrate towards the edge of the box but were subsequently pushed away again by the development of a plume in each corner. This sequence was then repeated with no signs of further breakdown of the convection pattern. Fig. 7(a) shows the temperature and stream function during this phase. At $t = 0.14$ (arrow 2) the perturbation was reapplied for a second time, and the system became much more time-dependent. However, it remained dominated by two major downwellings throughout this run. The lid was always mobile (in the sense that surface velocities were comparable with those in the interior) but the configurations of the individual 'plates'
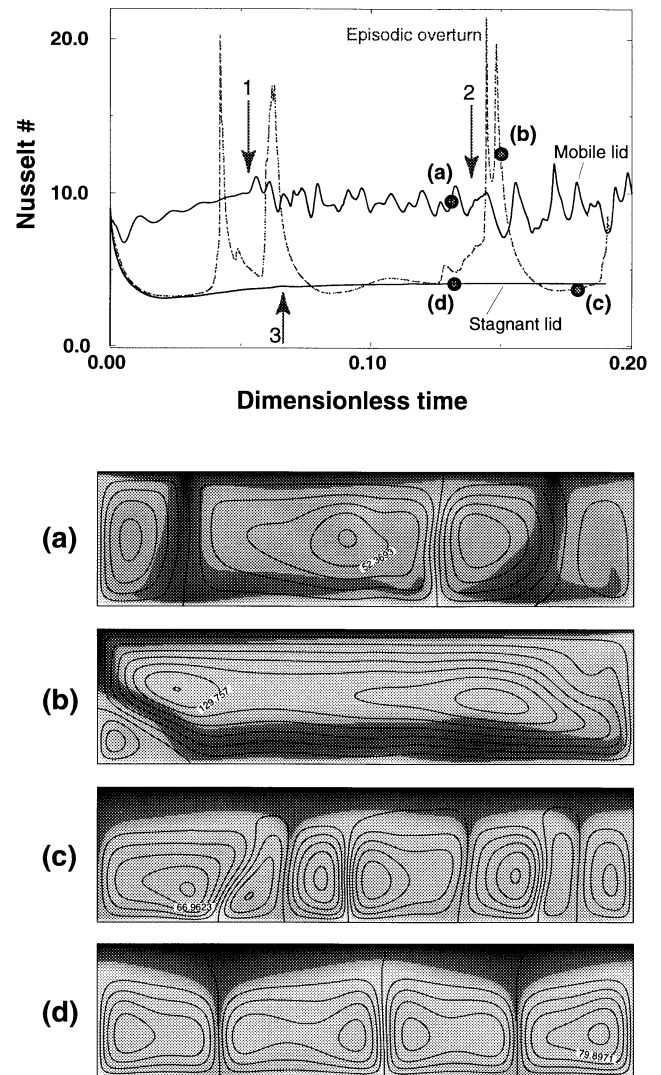

Figure 7. The effect of increasing aspect ratio on the three regimes. Nusselt number plot is equivalent to Fig. 3(a); the arrows indicate times at which longer-wavelength perturbations were introduced, the circles indicate the times of each snapshot. (a) Mobile-lid convection. (b) Episodic-overturn case as the upper boundary layer is in the middle of collapsing, and (c) as it reforms into a stagnant lid. (d) Stagnant-lid convection after perturbation.

© 1998 RAS, *GJI* **133**, 669–682

were frequently changed. The average Nusselt number was smaller (9.8) than the steady case with unit aspect ratio cells (10.7).

In the episodic-overturn run, considerably more complex time dependence was observed than in the 1×1 case with the same parameters. Initially the system evolved towards a stagnant lid quite smoothly, preserving the unit aspect ratio cells. However, the symmetry was destroyed after the first overturn, and the second collapse of the stagnant lid was more dramatic with the cold boundary layer pouring onto a single spot on the lower boundary. The anticipated overturn at $t \approx 0.1$ was not well recorded in the plot of the Nusselt number. Only the lower part of the stagnant lid collapsed, and the surface reflection of this was a small, broad rise in Nusselt number. Figs 7(b) and (c) show typical extremes of the mature system: a strong collapse of the stagnant lid into one corner of the box (b), in which the entire upper boundary moved coherently from right to left. Subsequently the presence of cold material on the lower boundary suppressed convection sufficiently that the stagnant lid redeveloped (c).

The stagnant-lid example (Fig. 7d) was almost unchanged from the original simulation in the 1×1 box. Perturbations (initial and at arrow 3) died away to give four nearly equal cells. The final Nusselt number was steady and agreed with that obtained in the 1×1 box.

SUMMARY AND DISCUSSION

The brittle properties of the lithosphere can be incorporated into mantle convection models by the introduction of a depth-dependent yield criterion limiting the maximum stress which can be supported by the rock. In taking this approach we are ignoring the size distribution and orientations of the faults responsible for brittle deformation. The problem then becomes one of viscoplastic flow, and can be simplified further to a highly non-linear, purely viscous flow. We have used a simple full multigrid approach to solving this problem efficiently and reliably when the viscosity is also highly temperature-dependent.

We observed competition between the temperature-dependent viscosity causing the cold boundary layer to stagnate, and brittle yielding within this boundary layer favouring mobilization. This led to three distinct regimes of behaviour dependent upon the magnitude of the yield criterion. When the lithosphere was very strong (high yield criterion), convection developed a stagnant lid with very low surface velocities and active circulation confined beneath the thick cold boundary layer. However, a weaker lithosphere fails before there is any possibility of stagnation and a quite different mode of convection ensues in which the lid is highly mobile, and actively circulates back into the interior. In this mobile-lid convection regime, much of the cold boundary layer is very viscous and does not deform, but brittle failure concentrates the large strain rates into narrow zones at the boundaries of the slowly deforming regions. Between these two end-member cases, we observed a third regime characterized by episodic overturns of an unstable stagnant lid. In some cases this episodic behaviour was a long-lived transient which eventually died away (usually leaving stagnant-lid convection) but in other cases the strength of the overturns showed no sign of diminishing with time.

The mobile-lid convection regime is interesting. The Nusselt number–Rayleigh number relationship is very well defined in this regime, and is almost entirely independent of the details of

the yield criterion which governs the onset of brittle behaviour; the same is true for average surface velocity. This indicates that the surface motions are governed by the properties of the interior part of the convection cell rather than by the rheology of the upper boundary layer. (In this sense it resembles convection with very weak temperature dependence; in the absence of brittle behaviour, as the viscosity contrast starts to increase, the surface velocities become limited by viscous resistance in the upper boundary layer.) A theoretical description of this convection regime based upon these observations is in good agreement with the numerical results.

Mercury, Mars and the Moon fall into the stagnant lid regime—they have very thick, strong lithospheres and convection is confined to the deep interior. At the opposite extreme, the Earth has very active surface motions in the form of plate tectonics which maintain a high heat flow and a relatively thin lithosphere within the oceanic regions. This is reminiscent of the mobile-lid regime. The puzzle is Venus. Although the radius, and probable bulk composition, are very similar to those of the Earth, there is almost no evidence for plate tectonics occurring on Venus (Kaula & Phillips 1981; Phillips *et al.* 1981; Solomon *et al.* 1991). Gravity and topography data are ambiguous and can be interpreted in terms of a thin lithosphere comparable to that of the Earth (Sandwell & Schubert 1992a,b; McKenzie 1994) or in terms of a very much thicker (~ 200 km), near-immobile lithosphere (Kiefer, Richards & Hager 1986; Kaula 1984, 1990a,b; Smrekar & Phillips 1991; Bindschadler, Schubert & Kaula 1992; Kucinskas & Turcotte 1994; Smrekar 1994; Moore & Schubert 1995; Solomatov & Moresi 1995). If the lithospheric thickness remains a puzzle, a seemingly greater mystery is the fact that the age of the surface appears to be strikingly uniform, suggesting a dramatic global resurfacing event ~ 500 Myr ago (Schaber *et al.* 1992; Strom, Schaber & Dawson 1994), or at least a number of pulses of localized activity (Phillips *et al.* 1992). Turcotte (1993) suggested that the resurfacing history represented a sudden episode of 'plate tectonics' in which most or all of a thick lithosphere collapses under its own weight, founders into the deep mantle and disappears while a new lithosphere begins to grow by conductive cooling. Fowler & O'Brien (1996) and Solomatov & Moresi (1995) discussed how such a model might arise from a stagnant-lid convection regime if brittle behaviour was considered and the yield stress was exceeded in a significant fraction of the thick lithosphere. In this paper, we have shown that this mechanism does give rise to a collapse of the lid, and, if the friction coefficient is appropriate, the process can repeat. As the properties and thickness of the lithosphere are poorly constrained, it is not clear whether Venus is now permanently in the stagnant lid regime or if another overturn will occur in the future.

For Venus to exhibit this type of behaviour, but not the Earth, suggests that either the driving forces from mantle convection are smaller in Venus, that is radiogenic heating is weaker, or the strength of the lithosphere is significantly higher. One possibility is that the presence of water at the Earth's surface is responsible for reducing the friction coefficient on faults to a low enough value that the surface can become mobile; the important but uncertain role of hydrous fluids in the evolution of faults and their strength as summarized by Hickman, Sibson & Bruhn (1995). The relative strengths of faults on the Earth and Venus have been examined by Foster & Nimmo (1996) who compared the morphology of grabens

in the East African Rift System with similar structures in the rifts of Beta Regio on Venus. Despite the fact that the lithosphere has a similar elastic thickness in each location, half-graben widths in Beta Regio are up to three times greater than in East Africa. This implies that the bounding faults of the structures on Venus have to be significantly stronger than the corresponding faults on Earth.

Our theory tentatively predicts that a mobile-lid regime would develop in the Earth if the friction coefficient of a continuum representation of faults is less than approximately $\mu = 0.03\text{--}0.13$ and that the resulting surface velocities would be controlled by the mantle viscosity and not by this frictional resistance—energy release would occur in a distributed zone in the mantle rather than being directly associated with individual faults. Although $\mu = 0.03\text{--}0.13$ is a low range, it seems to be consistent with the lack of heat-flow anomalies associated with major faults (Brune, Henyey & Roy 1969; Henyey & Wasserburg 1971; Lachenbruch & Sass 1973, 1980), and the low stress drops associated with earthquakes on rapidly slipping faults (Kanamori 1994). Zhong & Gurnis (1994, 1996) have shown, using large-scale convection models with embedded faults, that trench topography can be used to provide an independent constraint on the resisting stresses at plate boundaries. In 3-D modelling they also used observed plate kinematics to provide additional information on fault strengths in their computations. They concluded that frictional forces resisting subduction and motion on transform faults are relatively small, that is faults are weak.

Although faults may be weak, rocks in general are not. Measurements in the laboratory predict relatively large friction coefficients (Byerlee 1970; Brace & Byerlee 1966), and the existence of long-lived mountainous topography indicates that the crust can support large loads (Jeffreys 1959; Artyushkov 1972). That faults are rendered weak as they accumulate slip, perhaps through the development of a gouge layer, is borne out by the data showing an increase in gouge-zone thickness as a function of slip (Scholtz 1987). History dependence of the friction coefficient is entirely missing from our formulation in which all material has a constant μ. It is likely to be of major importance during the initiation of new faults and during plate reorganizations when pre-existing crustal weaknesses might be reactivated in preference to the development of a new zone of brittle failure.

Another important difference between the Earth and the mobile-lid regime is that there is complete recycling of the lithosphere in the computations shown here. This occurs even when the viscosity contrast is large. Although the oceanic lithosphere does get destroyed in this way, there is still Archaean lithosphere in continental areas which has somehow escaped this erosion and recycling process. In the Earth the mobile-lid regime may apply in one region, with other areas in a transitional state or even stagnant, possibly maintained by the presence of continental crust. Clearly it will be interesting to introduce chemical heterogeneity into this system to examine the evolution of the subcontinental lithosphere in the presence of mobile oceanic lithosphere.

Is mobile-lid convection a good model of plate tectonics? In some important aspects, this mode of convection does resemble plate tectonics. For example, the upper boundary layer moves quite freely with deformation restricted to the weakened margins of broad zones where high viscosity dominates; heat transport is relatively efficient due to the circulation of the cold material back into the interior; the sizes of the slowly deforming surface patches are self-determining with the aspect ratio of the flow often relatively large; and the stress balance between lithosphere and mantle is developed self-consistently. On the other hand, there are equally important aspects of plate tectonics which are completely absent from our models: the plate boundaries are not persistent but may reorganize at any time (and heal perfectly); the weak margins are still more broad than those on the Earth and are perfectly isotropic, unlike faults; downwellings are two-sided, not asymmetric as observed in subduction; in three dimensions there is no mechanism for producing and retaining transform structures, which are a key to stabilizing the long-term motions of the plates (Richards & Engebretson 1994). However, this fuzzy picture of plate tectonics is essentially what we expected when we made the initial assumptions about the rheology and given the relatively low resolution of our computations. We have demonstrated that the techniques used in finer-scale crustal modelling are useful for the incorporation of plates into mantle flow in a self-consistent manner. To progress it will be necessary to tackle the problem of the very different length scales at which mantle and crustal processes need to be studied. At the very least, dramatic grid refinement will be needed in the lithosphere to resolve plate boundaries—preferably adapting the grid density as the boundaries evolve. To incorporate the history requirement for the generation of realistic faults demands high resolution, and a Lagrangian frame of reference is also likely to be needed.

REFERENCES

Artyushkov, E.V., 1972. Stresses in the lithosphere caused by crustal thickness inhomogeneities, *J. geophys. Res.,* **78,** 7675–7708.

Beaumont, C., Fullsack, P. & Hamilton, J., 1994. Styles of crustal deformation in compressional orogens, in *Proc. 5th Int. Symp. Seism. Reflect. Prob. Contin. Marg.,* eds Clowes, R. & Green, A., *Tectonophysics,* **232,** 119–132.

Ben-Avraham, Z. & Lyakhovsky, V., 1992. Faulting processes along the northern Dead Sea transform and the Levant margin, *Geology,* **20,** 1139–1142.

Bercovici, D., 1993. A simple model of plate generation from mantle flow, *Geophys. J. Int.,* **114,** 635–650.

Bercovici, D., 1995. A source-sink model of the generation of plate tectonics from non-Newtonian mantle flow, *J. geophys. Res.,* **100,** 2013–2030.

Bindschadler, D., Schubert, G. & Kaula, W.M., 1992. Coldspots and hotspots: global tectonics and mantle dynamics of Venus, *J. geophys. Res.,* **97,** 13 495–13 532.

Bird, P., 1989. New finite element techniques for modeling deformation histories of continents with stratified temperature dependent rheology, *J. geophys. Res.,* **94,** 3967–3990.

Bird, P., 1997. Testing hypotheses on plate-driving mechanisms with global models of the faulted lithosphere, *J. geophys. Res.,* submitted.

Booker, J.R., 1976. Thermal convection with strongly temperature dependent viscosity, *J. Fluid Mech.,* **76,** 741–754.

Brace, W.F. & Byerlee, J.D., 1966. Stick-slip as a mechanism for earthquakes, *Science,* **153,** 990–992.

Braun, J. & Beaumont, C., 1987. Styles of continental rifting: results from dynamic models of lithospheric extension, in *Sedimentary Basins and Basin-Forming Mechanisms,* pp. 241–258, eds Beaumont, C. & Tankard, A.J., Can. Soc. Petrol. Geol.

Brooks, A.N. & Hughes, T.J.R., 1982. Streamline Upwind/Petrov-Galerkin formulations for convection dominated flows with particular emphasis on the incompressible Navier-Stokes equations, *Computer Methods appl. Mech. Eng.,* **32,** 199–259.

Brune, J.N., Henyey, T.L. & Roy, R.F., 1969. Heat flow, stress and the rate of slip along the San Andreas fault, California, *J. geophys. Res.,* **74,** 3821–3827.

Byerlee, J., 1968. The brittle-ductile transition in rocks, *J. geophys. Res.,* **73,** 4741–4750.

Byerlee, J.D., 1970. Static and kinetic friction of granite at high normal stress, *Int. J. Rock Mech. Min. Soc.,* **7,** 577–582.

Chopelas, A. & Boehler, R., 1989. Thermal expansion measurements at very high pressure, systematics, and a case for a chemically homogeneous mantle, *Geophys. Res. Lett.,* **16,** 1347–1350.

Christensen, U., 1984. Convection with pressure- and temperature-dependent non-Newtonian rheology, *Geophy. J. R. astr. Soc.,* **77,** 343–384.

Christensen, U.R., 1983. Convection in a variable viscosity fluid: Newtonian versus power law, *Earth Planet. Sci. Lett.,* **64.**

Cserepes, L., 1982. Numerical studies of non-Newtonian mantle convection, *Phys. Earth. planet. Inter.,* **30,** 49–61.

Davaille, A. & Jaupart, C., 1993. Thermal convection in lava lakes, *Geophys. Res. Lett.,* **20,** 1827–1830.

Davaille, A. & Jaupart, C., 1994. Onset of thermal convection in fluids with temperature dependent viscosity: application to the oceanic mantle, *J. geophys. Res.,* **99,** 19 853–19 866.

Davies, G., 1988. Role of the lithosphere in mantle convection, *J. geophys. Res.,* **93,** 10 451–10 466.

Davies, G.F., 1989. Mantle convection model with a dynamic plate: topography, heat flow and gravity anomalies, *Geophys. J. Int.,* **98,** 461–464.

DeMets, C., Gordan, R.G., Argus, D.F. & Stein, S., 1990. Current plate motions, *Geophys. J. Int.,* **101,** 425–478.

Dunbar, J.A. & Sawyer, D.S., 1989. How pre-existing weaknesses control the style of continental breaking, *J. geophys. Res.,* **94,** 7278–7292.

Foster, A. & Nimmo, F., 1996. Comparisons between the rift systems of East Africa, Earth and Beta Regio, Venus, *Earth planet. Sci. Lett.,* **143,** 183–195.

Fowler, A., 1985a. Boundary layer theory and subduction, *J. geophys. Res.,* **98,** 21 997–22 005.

Fowler, A.C., 1985b. Fast thermoviscous convection, *Stud. appl. Math.,* **72,** 189–219.

Fowler, A.C. & O'Brien, S.B.G., 1996. A mechanism for episodic subduction on Venus, *J. geophys. Res.,* **101,** 4755–4763.

Frank-Kamenetskii, D.A., 1969. *Diffusion and Heat Transfer in Chemical Kinetics,* Plenum, New York, NY.

Fullsack, P., 1995. An arbitrary Lagrangian–Eulerian formulation for creeping flows and its application in tectonic models, *Geophys. J. Int.,* **120,** 1–23.

Gable, C.W., O'Connell, R.J. & Travis, B.J., 1991. Convection in three dimensions with surface plates: generation of toroidal flow, *J. geophys. Res.,* **96,** 7205–7223.

Gurnis, M., 1988. Large scale mantle convection and the aggregation and dispersal of supercontinents, *Nature,* **332,** 695–699.

Hager, B.H. & O'Connel, R.J., 1981. A simple global model of plate dynamics and mantle convection, *J. geophys. Res.,* **86,** 4843–4867.

Henyey, T.L. & Wasserburg, G.J., 1971. Heat flow near major strike slip faults in California, *J. geophys. Res.,* **76,** 7924–7946.

Hess, H.H., 1962. History of ocean basins, in *Petrologic Studies: a Volume in Honor of A.F. Buddington,* pp. 559–620, eds Engel, A.E.J., James, H.L. & Leonard, B.F., Geol. Soc. Am., New York, NY.

Hickman, S., Sibson, R. & Bruhn, R., 1995. Introduction to special session: mechanical involvement of fluids in faulting, *J. geophys. Res.,* **100,** 12 831–12 840.

Holmes, A., 1931. Radioactivity and earth movements, *Trans. Geol. Soc. Glasgow,* **18,** 559–606.

Isacks, B., Oliver, J. & Sykes, L.R., 1968. Seismology and the new global tectonics, *J. geophys. Res.,* **73,** 5855–5899.

Jeffreys, H., 1959. *The Earth,* Cambridge University Press, Cambridge.

Kanamori, H., 1994. Mechanics of earthquakes, *Ann. Rev. Earth planet. Sci.,* **22,** 207–237.

Karato, S. & Wu, P., 1993. Rheology of the upper mantle: a synthesis, *Science,* **260,** 771–778.

Kaula, W.M., 1984. Tectonic contrasts between Venus and the Earth, *Geophys. Res. Lett.,* **11,** 35–37.

Kaula, W.M., 1990a. Mantle convection and crustal evolution on Venus, *Geophys. Res. Lett.,* **17,** 1401–1403.

Kaula, W.M., 1990b. Venus: a contrast in evolution to Earth, *Science,* **247,** 1191–1196.

Kaula, W.M. & Phillips, R.J., 1981. Quantitative tests for plate tectonics on Venus, *Geophys. Res. Lett.,* **8,** 1187–1190.

Kiefer, W.S., Richards, M.A. & Hager, B.H., 1986. A dynamic model of Venus's gravity field, *Geophys. Res. Lett.,* **13,** 14–17.

King, S.D. & Hager, B.H., 1990. The relationship between plate velocity and trench viscosity in Newtonian and power-law subduction calculations, *Geophys. Res. Lett.,* **17,** 2409–2412.

Koptizke, U., 1979. Finite element convection models: comparison of shallow and deep mantle convection and temperatures in the mantle, *J. Geophys.,* **46,** 97–121.

Kucinskas, A.B. & Turcotte, D.L., 1994. Isostatic compensation of equatorial highlands on Venus, *Icarus,* **112,** 42–54.

Lachenbruch, A.H. & Sass, J.H., 1973. *Thermomechanical Aspects of the San Andreas Fault System,* Stanford University Press, Stanford, CA.

Lachenbruch, A.H. & Sass, J.H., 1980. Heat flow and energetics of the San Andreas fault zone, *J. geophys. Res.,* **85,** 6185–6222.

Lithgow-Bertelloni, C. & Richards, M.A., 1995. Cenozoic plate driving forces, *Geophys. Res. Lett.,* **22,** 1317–1320.

Lyakhovsky, V., Podlachikov, Y. & Poliakov, A.N.B., 1993. A rheological model of a fractured solid, *Tectonophysics,* **226,** 187–198.

McKenzie, D., 1994. The relationship between topography and gravity on Earth and Venus, *Icarus,* **112,** 55–88.

McKenzie, D. & Bickle, M.J., 1988. The volume and composition of melt generated by extension of the lithosphere, *J. Petrol.,* **29,** 625–679.

McKenzie, D.P., 1977. Surface deformation, gravity anomalies and convection, *Geophy. J. R. astr. Soc.,* **48,** 211–238.

Minster, J.B. & Jordan, T.H., 1978. Present-day plate motions, *J. geophys. Res.,* **83,** 5331–5354.

Moore, W.B. & Schubert, G., 1995. Lithospheric thickness and mantle/lithosphere density contrast beneath Beta Regio, Venus, *Geophys. Res. Lett.,* **22,** 429–432.

Moresi, L. & Solomatov, V.S., 1995. Numerical investigations of 2D convection with extremely large viscosity contrasts, *Phys. Fluids,* **7,** 2154–2162.

Morris, S. & Canright, D., 1984. A boundary layer analysis of Bénard convection in a fluid of strongly temperature dependent viscosity, *Phys. Earth. planet. Inter.,* **36,** 355–373.

Nataf, H.C. & Richter, F.M., 1982. Convection experiments in fluids with highly temperature-dependent viscosity and the thermal evolution of the planets, *Phys. Earth. planet. Inter.,* **29,** 320–329.

Olson, P. & Corcos, G.M., 1980. A boundary layer model for mantle convection with surface plates, *Geophy. J. R. astr. Soc.,* **62,** 195–219.

Parmentier, E.M., Turcotte, D.L. & Torrance, K.E., 1976. Studies of finite amplitude, non-Newtonian thermal convection with application to convection in the Earth's mantle, *J. Geophys. Res.,* **81,** 1839–1846.

Phillips, R.J., Kaula, W.M., McGill, G.E. & Malin, M.C., 1981. Tectonics and evolution of Venus, *Science,* **212,** 879–887.

Phillips, R.J., Rambertas, R.F., Arvidson, R.E., Sarkar, I.C., Herrick, R.R., Izenberg, N. & Grimm, R.E., 1992. Impact craters and Venus resurfacing history, *J. Geophys. Res.,* **97,** 15 923–15 948.

Poliakov, A.N.B. & Herrmann, H.J., 1994. Self-organized criticality of plastic shear bands in rocks, *Geophys. Res. Lett.,* **21,** 2143–2146.

Ratcliff, J.T., Schubert, G. & Zebib, A., 1995. Three-dimensional variable viscosity convection of an infinite Prandtl number Boussinesq fluid in a spherical shell, *Geophys. Res. Lett.,* **22,** 2227–2230.

Ricard, Y. & Vigny, C., 1989. Mantle dynamics with induced plate tectonics, *J. geophys. Res.,* **94,** 17 543–17 559.

Richards, M.A. & Engebretson, D.C., 1994. Transform faults—a guiding force of plate tectonics, *EOS, Trans. Am. geophys. Un.,* **75,** 63.

Sandwell, D.T. & Schubert, G., 1992a. Evidence for retrograde lithospheric subduction on Venus, *Science,* **257,** 766–770.

Sandwell, D.T. & Schubert, G., 1992b. Flexural ridges, trenches and outer rises around coronae on Venus, *J. geophys. Res.,* **97,** 16 069–16 083.

Schaber, G.G. *et al.,* 1992. Geology and distribution of impact craters on Venus: what are they telling us?, *J. geophys. Res.,* **97,** 13 257–13 301.

Schmeling, H. & Jacoby, W.R., 1981. On modelling the lithosphere in mantle convection with nonlinear rheology, *J. Geophys.,* **50,** 89–100.

Scholtz, C.H., 1987. Wear and gouge formation in brittle faulting, *Geology,* **15,** 309–34.

Sleep, N., 1975. Stress and flow beneath island arcs, *Geophys. J. R. astr. Soc.,* **42,** 827–857.

Smrekar, S. & Phillips, R., 1991. Venusian highlands: geoid to topography ratios and their implications, *Earth planet. Sci. Lett.,* **107,** 582–597.

Smrekar, S.E., 1994. Evidence for active hotspots on Venus from analysis of Magellan gravity data, *Icarus,* **112,** 2–26.

Solomatov, V.S., 1995. Scaling of temperature- and stress-dependent viscosity convection, *Phys. Fluids,* **7,** 266–274.

Solomatov, V.S. & Moresi, L., 1995. Stagnant lid convection on Venus, *J. geophys. Res.,* **101,** 4737–4753.

Solomatov, V.S. & Moresi, L., 1997. Three regimes of mantle convection with non-Newtonian viscosity and stagnant lid convection on the terrestrial planets, *Geophys. Res. Lett.,* **24,** 1907–1910.

Solomon, S.C., Head, J.W., Kaula, W.M., McKenzie, D., Parsons, B., Phillips, R.J., Schubert, G. & Talwani, M., 1991. Venus tectonics: initial analysis from Magellan, *Science,* **252,** 297–312.

Strom, R.G., Schaber, G.G. & Dawson, D.D., 1994. The global resurfacing of Venus, *J. geophys. Res.,* **99,** 10 899–10 926.

Tackley, P.J., 1993. Effects of strongly variable viscosity on time-dependent, three-dimensional models of mantle convection, *Geophys. Res. Lett.,* **20,** 2187–2190.

Torrance, K.E. & Turcotte, D.L., 1971. Thermal convection with large viscosity variations, *J. Fluid Mech.,* **47,** 113–125.

Turcotte, D.L., 1993. An episodic hypothesis for Venusian tectonics, *J. geophys. Res.,* **98,** 17 061–17 068.

Turcotte, D.L. & Oxburgh, E.R., 1967. Finite amplitude convection cells and continental drift, *J. Fluid Mech.,* **28,** 29–42.

Vermeer, P.A., 1990. The orientation of shear bands in biaxial tests, *Géotechnique,* **40,** 223–236.

Weinstein, S.A. & Olson, P.L., 1992. Thermal convection with non-Newtonian plates, *Geophys. J. Int.,* **111,** 515–530.

White, R.S., 1993. Melt production rates in mantle plumes, *Phil. trans. R. Soc. Lond.,* A, **342,** 137–153.

Zhong, S. & Gurnis, M., 1994. Controls on trench topography from dynamic models of subducted slabs, *J. Geophys. Res.,* **99,** 15 683–15 696.

Zhong, S. & Gurnis, M., 1995. Mantle convection with plates and mobile, faulted plate margins, *Science,* **267,** 838–843.

Zhong, S. & Gurnis, M., 1996. Interaction of weak faults and non-Newtonian rheology produces plate tectonics in a 3D model of mantle flow, *Nature,* **383,** 245–247.